Theory of crystal-field splitting and orbit-lattice coupling of rare-earth impurities in noble metals

1990 J. Phys.: Condens. Matter 2 577

(http://iopscience.iop.org/0953-8984/2/3/006)

J. Phys.: Condens. Matter 2 (1990) 577–594. Printed in the UK

Theory of crystal-field splitting and orbit–lattice coupling of rare-earth impurities in noble metals

G G Khaliullin and S V Buzukin
Physicotechnical Institute of the Academy of Sciences of the USSR, Kazan 420029, USSR

Received 20 February 1989

Abstract. The origin of the 4f state splitting of rare-earth ion in noble metals (Cu, Ag and Au) has been investigated. The contributions to the crystal-field and orbit–lattice coupling parameters from

(i) the potential of host ions screened by the conduction electrons,
(ii) the screening effects due to the local 5d density and
(iii) the covalent mixing of the 4f and 5d states with the s and d bands

have been calculated. As a result, good agreement with experimental values of the interaction parameters was obtained for the whole of the noble-metal series. The possibilities of different experimental techniques for unambiguous determination of the crystal-field parameters have also been discussed.

1. Introduction

Magnetic properties of a crystal containing rare-earth (RE) ions are mainly determined by the ion–lattice interaction, leading to the 4f-state splitting. For a regular ion environment, the splitting is described by a crystal-field (CF) Hamiltonian with appropriate symmetry. Additional interaction with the crystal distortion is conventionally known as an orbit–lattice (OL) coupling. Neutron scattering [1], magnetic susceptibility [2], electron paramagnetic resonance (EPR) [3–5], Mössbauer absorption [6] and other experiments have provided some information on the CF parameters in a number of metals. Recently the results of investigations of OL coupling in dilute alloys by magnetostriction measurements [7] and EPR analysis on thin films [8] and bulk samples [9] have been reported. The data obtained show the naive point-charge model to be inappropriate even for qualitative conclusions. Various mechanisms, namely the 5d virtual bound-state effects [2], the covalency between the 4f electrons and conduction band [10] and the screening of the potential of host ions by the conduction electrons [11] have already been discussed. However, up to now there has been no appropriate microscopic theory of the RE ion–lattice interaction in metals. Moreover, the relative roles of various interaction mechanisms available are not quite clear.

Therefore, combined analysis of the possible CF sources in some metallic systems appears to be of interest. In the present treatment, dilute alloys based on noble metals

0953-8984/90/030577 + 18 $03.50

(Cu, Ag and Au) are considered. These alloys have the FCC lattice structure. It is well known that the cubic CF Hamiltonian may be written [12]

$$\mathcal{H}_{CF} = C_4\beta_J(O_4^0 + 5O_4^4) + C_6\gamma_J(O_6^0 - 21O_6^4) \tag{1}$$

where C_4 and C_6 are the fourth- and sixth-order CF parameters, β_J and γ_J are the Stevens factors, and O_n^m are the angular momentum operators. The interaction between the RE ion and crystal distortion is governed by the OL Hamiltonian [13]

$$\mathcal{H}_{OL} = \sum_{n\Gamma\alpha} V_\Gamma^{(n)} O_{\Gamma\alpha}^{(n)} e_{\Gamma\alpha} \tag{2}$$

where $V_\Gamma^{(n)}$ are the OL parameters, $O_{\Gamma\alpha}^{(n)}$ and $e_{\Gamma\alpha}$ are linear combinations of the nth-order Stevens operators and the strain tensor components, respectively, transforming as the αth component of the irreducible representation Γ of the point-symmetry group. For a cubic crystal, there are two principal types of deformation: tetragonal (Γ_{3g}) and trigonal (Γ_{5g}) with

$$e_{3g\theta} = \tfrac{1}{2}(2e_{zz} - e_{xx} - e_{yy}) \qquad e_{5g\xi} = e_{yz}$$
$$e_{3g\nu} = (3^{1/2}/2)(e_{xx} - e_{yy}) \qquad e_{5g\eta} = e_{xz}$$
$$e_{ii} = \varepsilon_{ii} \qquad e_{5g\zeta} = e_{xy} = \varepsilon_{xy} + \varepsilon_{yx}$$

where ε_{ij} are the displacement tensor components. The corresponding second-order operators are

$$O_{3g\theta}^{(2)} = \tfrac{1}{2}[3J_z^2 - J(J+1)] \qquad O_{5g\xi}^{(2)} = (1/4\mathrm{i})(J_+^2 - J_-^2).$$

Thus the interaction between the impurity RE ion and lattice is characterised by the set of parameters C_4, C_6, $V_{3g}^{(n)}$, and $V_{5g}^{(n)}$, $n = 2, 4, 6$.

The paper is organised as follows. After qualitative discussion of possible mechanisms of the 4f-electron–lattice interaction (§ 2.1), the expressions for their contributions to the parameters of interaction are obtained (§§ 2.2–2.4). The experimental values of the parameters are given in § 3 and are compared with our theoretical estimates. The conclusions are summarised in § 4.

2. Theory

2.1. Origin of the crystal field

Among possible sources of the 4f-state splitting, the host ions' potential seems to be the most obvious. However, this potential is affected by the conduction electrons in metals, and the effective ion charge depends on the competition between two opposite tendencies. First, free electrons tend to screen the ion charge and, secondly, the orthogonality between the wavefunctions of the band and core states leads to the removal of the conduction electrons from the core region. Hence the host ion should be characterised by a pseudopotential. In [11] the CF parameters were calculated using the bare pseudopotential $v^0(g) \propto g^{-2}\exp(-g^2b^2/4)$ (b is the cut-off parameter). The same pseudopotential has also been employed for analysis of the OL coupling [14]. For all b-values and different types of screening, the ion–lattice interaction parameters have been found to be reduced in magnitude with respect to the point-charge model values and to change the signs in some cases. A somewhat different approach to the screening has been

performed in [15]. From a calculation in real space using the Coulomb potential the CF parameters were found to be enhanced by screening due to the decrease in the next-nearest-neighbour contribution with the sign opposite to that of the nearest-neighbour contribution.

Covalent mixing of the 4f states with the conduction electrons makes the transitions within the 4f shell possible via the band. The splitting caused by such processes may also be represented by the action of the effective crystalline potential. Strong Coulomb repulsion between the 4f electrons must be taken into consideration and the Anderson model [16] seems to be convenient for calculations. In [10] C_4 was estimated to be about $\pm 100\,\mathrm{cm}^{-1}$. It should be expected that the covalency contributes to OL coupling too, because the covalent coupling of the 4f electrons with ligand d orbitals is strongly modulated by lattice distortion. At the same time, the modulation of the coupling with the s band may be weak.

The part of anisotropic potential seen by the 4f electrons should be attributed to the existence of the impurity 5d level above the Fermi level. Usually this mechanism is described in terms of the virtual bound-state model (see, e.g., [17]). Within this model, covalent mixing of the 5d states with the s band permits free electrons to be localised partially in the 5d states. This may be regarded as the 5d-level broadening. The occupation numbers of 5d t_{2g} and 5d e_g states are unequal, because the states are split by the cubic CF. Thus, they produce an anisotropic Coulomb potential on the 4f electrons. If a crystal is deformed, an additional splitting of t_{2g} and e_g states arises, which changes their occupation numbers. Hence the lattice distortion modulates the 4f–5d Coulomb interaction and shifts the energies of the 4f electrons. However, as will be seen below, this treatment is not complete and the covalent mixing with ligand d orbitals is of great importance. The wavefunction of the d orbital may be written as

$$\Psi_\mathrm{d} = \Psi_\mathrm{d}^0 + [V_{5\mathrm{d},\mathrm{d}}/(\varepsilon_\mathrm{d} - \varepsilon_{5\mathrm{d}})]\Psi_{5\mathrm{d}}$$

where $V_{5\mathrm{d},\mathrm{d}}$ is the hopping integral. Then the relevant matrix element of the impurity–ligand Coulomb interaction is

$$\begin{aligned}\langle\Psi_\mathrm{d}, \Psi_{4\mathrm{f}}|1/r_{12}|\Psi_{4\mathrm{f}}, \Psi_\mathrm{d}\rangle &= \langle\Psi_\mathrm{d}^0, \Psi_{4\mathrm{f}}|1/r_{12}|\Psi_{4\mathrm{f}}, \Psi_\mathrm{d}^0\rangle \\ &+ [V_{5\mathrm{d},\mathrm{d}}^2/(\varepsilon_\mathrm{d} - \varepsilon_{5\mathrm{d}})^2]\langle\Psi_{5\mathrm{d}}, \Psi_{4\mathrm{f}}|1/r_{12}|\Psi_{4\mathrm{f}}, \Psi_{5\mathrm{d}}\rangle \\ &+ \{[V_{5\mathrm{d},\mathrm{d}}/(\varepsilon_\mathrm{d} - \varepsilon_{5\mathrm{d}})]\langle\Psi_\mathrm{d}^0, \Psi_{4\mathrm{f}}|1/r_{12}|\Psi_{4\mathrm{f}}, \Psi_{5\mathrm{d}}\rangle + \mathrm{CC}\}. \qquad (3)\end{aligned}$$

The first term on the right-hand side in equation (3) should be attributed to the host ion potential. The second term is the 5d-electron potential, the quantity $V_{5\mathrm{d},\mathrm{d}}^2/(\varepsilon_\mathrm{d} - \varepsilon_{5\mathrm{d}})^2$ being the 5d-state occupation number due to the covalent coupling with ligands. This mechanism contributes to both the CF splitting and the OL coupling of the 4f electrons. The last term in equation (3) describes the potential produced by the charge density located in the impurity–ligand region. It is reasonable to call this additional density a covalent charge.

2.2. *Lattice potential screening by free electrons*

The simple point-charge approximation gives

$$\begin{aligned}C_4 &= \tfrac{7}{32}(Z\langle r^4\rangle/d^5)(1 + \sigma_4) \qquad C_6 = \tfrac{39}{256}(Z\langle r^6\rangle/d^7)(1 + \sigma_6) \\ V_{5g}^{(2)} &= -V_{3g}^{(2)} = (3Z\langle r^2\rangle\alpha_J/d^3)(1 + \sigma^{(2)}) \qquad (4)\end{aligned}$$

where α_J is the Stevens factor, $\langle r^n \rangle$ is the nth moment of the 4f orbital, Z is the host ion valency and d is the distance between the RE ion and its nearest neighbours. The next-nearest-neighbour contributions to the interaction parameters are $\sigma^{(2)} = -0.4$, $\sigma_4 = -0.25$ and $\sigma_6 = -0.03$.

To take into account the spatial extent of a host ion and screening properties of a free-electron gas, the point-charge potential has to be substituted by the ionic pseudopotential $v(g) = v^0(g)/\varepsilon(g)$ (here $\varepsilon(g)$ is the dielectric screening function). We use the empty-core approximation and the Hartree screening (see, e.g., [18]). It is convenient to represent the screened potential $V(\boldsymbol{r})$ as a sum over the reciprocal lattice vectors g:

$$V(r) = \sum_g \exp(i\boldsymbol{g}\cdot\boldsymbol{r})\, v(g). \tag{5}$$

This can be rewritten in the form

$$V(r) = V_p(\boldsymbol{r}) - \sum_g \exp(i\boldsymbol{g}\cdot\boldsymbol{r})\, v(g)[\varepsilon(g) - 1] \tag{6}$$

having better convergence. Here $V_p(r)$ is the unscreened point-ions' potential. To present the interaction in the usual form (equations (1) and (2)), one should expand $V(\boldsymbol{r})$ about the RE ion in terms of spherical harmonics and average the coefficients of the expansion over a radial function $R_{4f}(r)$. In order to clarify the continuous dependence of the screening on the 4f-orbital extent we use $R_{4f}(r) = Ar^3\exp(-\alpha r)$ and obtain as the result

$$C_4 = \tfrac{7}{32}(Z\langle r^4\rangle/d^5)(1 + \sigma_4 + \lambda_4) \qquad C_6 = \tfrac{39}{256}(Z\langle r^6\rangle/d^7)(1 + \sigma_6 + \lambda_6)$$

$$V_{3g}^{(2)} = -(3Z\langle r^2\rangle\alpha_J/d^3)(1 + \sigma^{(2)} + \lambda_{3g}^{(2)}) \qquad V_{5g}^{(2)} = (3Z\langle r^2\rangle\alpha_J/d^3)(1 + \sigma^{(2)} + \lambda_{5g}^{(2)})$$

$$\lambda_4 = \tfrac{9}{5}\sum_g \gamma(1 - \tfrac{3}{11}y)\xi d^2 g^2(g_3^4 - 3g_1^2 g_2^2)$$

$$\lambda_6 = -\tfrac{2}{715}\sum_g \gamma\xi d^4 g^2(g_3^6 - 15g_1^2 g_2^4 + 30g_1^2 g_2^2 g_3^2)$$

$$\lambda_{3g}^{(2)} = -\sum_g \gamma G_1[6\xi g_1^2 g_2^2 - \zeta(g_3^4 - g_1^2 g_2^2)] \qquad \lambda_{5g}^{(2)} = 3\sum_g \gamma G_1(\xi g_3^4 - \zeta g_1^2 g_2^2)$$

$$\gamma = (16 \times 2^{1/2} k_F/189a_0)[(1 + y)^{-8}/g^6\varepsilon(g)] \qquad \xi = \chi\cos(gr_c) \tag{7}$$

$$\zeta = gr_c\sin(gr_c) + \cos(gr_c)(2\chi G_2 + \eta/\varepsilon(g))$$

$$\chi = \tfrac{1}{2} + [(1 - x^2)/4x]\ln|(1 + x)/(1 - x)|$$

$$\eta = \tfrac{1}{2} + [(3 - x^2)/4x]\ln|(1 + x)/(1 - x)| \qquad x = g/2k_F$$

$$G_1 = 21 - 30y + 5y^2$$

$$G_2 = (198 - 220y + 30y^2)y/(21 - 9y - 25y^2 + 5y^3) \qquad y = (g/2\alpha)^2$$

where r_c is the ion core radius and k_F is the Fermi wavevector.

The sums (7) over the reciprocal lattice converge rapidly. The screening factors λ depend on three parameters: α, k_F and r_c. The 4f-orbital radius can be estimated by fitting to the averages $\langle r^n\rangle_{4f}$ calculated in [19], e.g. for an Er^{3+} ion $\alpha \simeq 5$ au^{-1}. The values

Table 1. Factors of the host ion field screening for an Er impurity. Values of the Fermi momentum k_F and core radius r_c used in calculations are taken from [18].

	4f electron				5d electron						
Host	λ_4	λ_6	$\lambda_{5g}^{(2)}$	$\lambda_{5g}^{(2)}$	λ_4	$\lambda_{3g}^{(2)}$	$\lambda_{5g}^{(2)}$	$\lambda_{3g}^{(4)}$	$\lambda_{5g}^{(4)}$	k_F (au^{-1})	r_c (au)
Cu	0.00	0.08	−0.03	−0.12	0.04	−0.02	0.06	0.05	0.04	0.72	1.27
Ag	0.18	0.24	−0.06	0.37	0.10	−0.03	0.25	0.09	0.10	0.64	1.68
Au	0.36	0.39	−0.08	0.89	0.16	−0.04	0.62	0.22	0.26	0.64	1.91

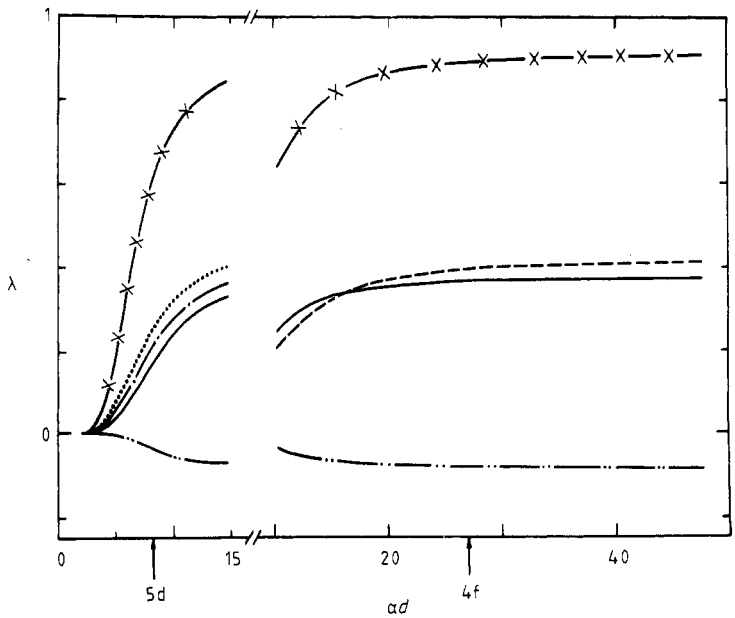

Figure 1. CF screening factors λ_4 (———), λ_6, (— — —), $\lambda_{3g}^{(2)}$ (— · · —), $\lambda_{5g}^{(2)}$ (— × —), $\lambda_{3g}^{(4)}$ (— · —) and $\lambda_{5g}^{(4)}$ (· · · ·) for Au are plotted against the reciprocal radii α of 4f and 5d orbitals of the RE ion. d is the nearest-neighbour distance. The arrows denote the values of $\alpha_{Er^{3+}}$.

of k_F and r_c used in the calculations are listed in table 1. We quote them from [18] (regarding the d-state radii determined therein as r_c). The obtained magnitudes of λ (equation (7)) are also presented in table 1. The behaviour of the screening factors as each of three parameters varies is shown in figures 1–3. Arrows denote the above values of α, k_F and r_c. It should be noted that the magnitude of the screening effect changes slightly on substitution of one RE ion by another (dependence on α). The divergences of $\lambda_\Gamma^{(2)}$ as a function of k_F occur because of the well known peculiarity of the free-electron susceptibility $\chi(q)$ at $q = 2k_F$. A strong dependence of the results on the core size r_c should be noted, the screening ($\lambda < 0$) being transformed to the anti-screening ($\lambda > 0$) with increase in r_c/d. This is due to an enhancement of the conduction electron removal from the host ion core, which increases the effective ion charge. Thus, in noble metals containing extended d orbitals, the anti-screening effect should be expected.

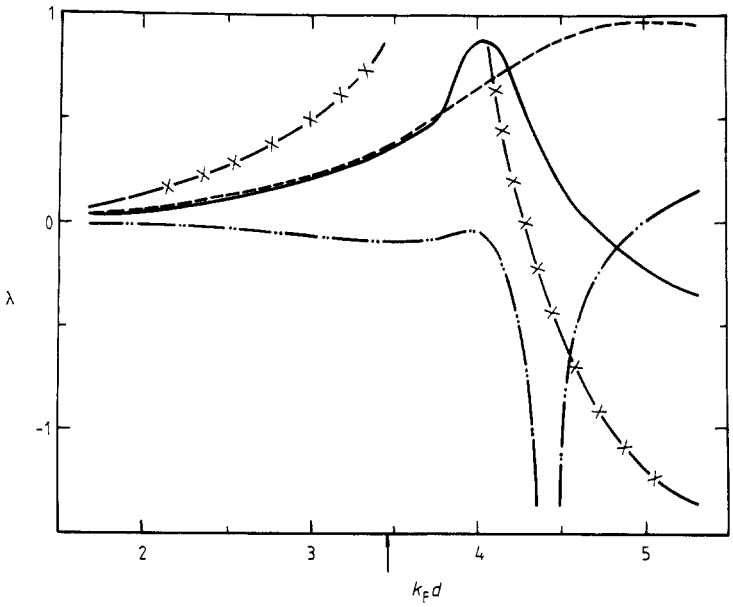

Figure 2. Screening factors for Au are plotted against the Fermi momentum k_F. The symbols have the same meanings as in figure 1. The arrow denotes the value of k_F(Au) listed in table 1.

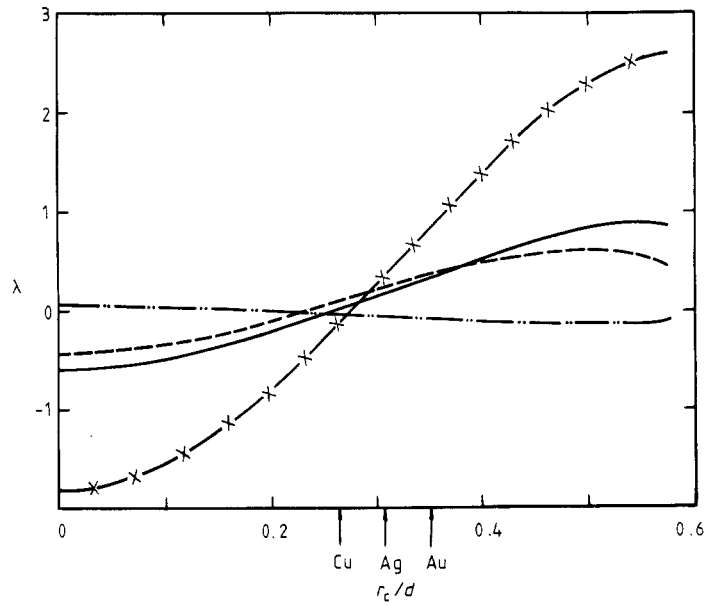

Figure 3. Screening factors are plotted against the host ion core radius r_c. The symbols have the same meanings as in figure 1. The arrows denote the values of r_c listed in table 1.

Screening of the CF seen by the 5d electrons of the RE ion is also of interest. The averages $\langle r^n\rangle_{5d}$ [20] are approximated well by $R_{5d}(r) = Ar^2\exp(-\alpha r)$ when $\alpha = 1.53$ au^{-1} for Er^{3+}. The corresponding λ(5d)-values calculated using formulae similar to (7) (we also take into account the fourth-order terms in the 5d-electron OL Hamiltonian) are presented in table 1. As an example, the dependences of the λ-values on the 5d-orbital radius are shown in figure 1.

In previous work [9] we have evaluated the screening of the impurity–lattice interaction using the Thomas–Fermi approximation. The interaction parameters have been found to decrease and to change the sign of $V_{3g}^{(2)}$. The results of the present paper show that the Friedel oscillations which have been ignored previously change the character of the screening significantly.

It should also be noted that no divergence of the sums over the reciprocal lattice, which has been discussed in [11], actually occurs. This divergence is due to unsuccessful expansion of $\exp(i\boldsymbol{g}\cdot\boldsymbol{r})$ in terms of a power series in $\boldsymbol{g}\cdot\boldsymbol{r}$. In turn, the results depend markedly on the choice of pseudopotential model. It is the empty-core approximation which leads to the anti-screening effect.

2.3. *Covalent mixing of the 4f states with the conduction band*

To calculate the covalent contribution, we use the Andersen model [16]. In our case, the Hamiltonian takes the form

$$\begin{aligned}
&\mathcal{H} = \mathcal{H}_{4f} + \mathcal{H}_{cond} + \mathcal{H}_1 \equiv \mathcal{H}_0 + \mathcal{H}_1 \\
&\mathcal{H}_{4f} = \varepsilon_f \sum_{m\sigma} \hat{n}_{m\sigma} + \mathcal{H}_{Coul} + \mathcal{H}_{so} \qquad \mathcal{H}_{cond} = \sum_{k\sigma} \varepsilon_k \hat{n}_{k\sigma} \qquad (8)\\
&\mathcal{H}_1 = \sum_{mk\sigma} (V_{mk} f_{m\sigma}^{+} c_{k\sigma} + V_{km} c_{k\sigma}^{+} f_{m\sigma})
\end{aligned}$$

where $c_{k\sigma}^{+}$ and $c_{k\sigma}$ are the operators which create and destroy conduction electron with wavevector $\boldsymbol{k}$, energy ε_k and spin σ; $f_{m\sigma}^{+}$ and $f_{m\sigma}$ are the corresponding 4f-electron operators; $\mathcal{H}_{Coul}$ and $\mathcal{H}_{so}$ terms correspond to the Coulomb and spin–orbit interactions within the 4f shell, respectively; V_{mk} is the hybridisation matrix element. An appropriate canonical transformation allows the off-diagonal operator $\mathcal{H}_1$ in (8) to be substituted by $\mathcal{H}_2$, satisfying the relation

$$\langle a|\mathcal{H}_2|b\rangle = \tfrac{1}{2}\langle a|\mathcal{H}_1[(E_a - \mathcal{H}_0)^{-1} + (E_b - \mathcal{H}_0)^{-1}]\mathcal{H}_1|b\rangle.$$

Here $|a\rangle$ and $|b\rangle$ are the eigenvectors of $\mathcal{H}_0$. After the averaging of $\mathcal{H}_2$ over the conduction band states, the extra operator acting within the 4f shell takes the form

$$\mathcal{H}_{cov} = \sum_{mm'k\sigma} V_{mk} V_{km'} \left(\frac{1 - n_k}{\varepsilon_- - \varepsilon_k} + \frac{n_k}{\varepsilon_+ - \varepsilon_k}\right) f_{m\sigma}^{+} f_{m'\sigma} \qquad (9)$$

where ε_+ is the energy required for transferring an electron from the Fermi level to the $4f^n$ configuration, ε_- is the energy required for removing an electron from the 4f shell. The difference between the $\varepsilon_\pm$ and ε_f levels is due to the strong Coulomb interaction between the 4f electrons. We do not deal with the ions on the edges of the RE series (Ce and Yb), for which one of these levels may closely approach the Fermi level. In addition, ε_+ processes are predominant for heavy RE ions. The operator $\mathcal{H}_{cov}$ (9) contains the

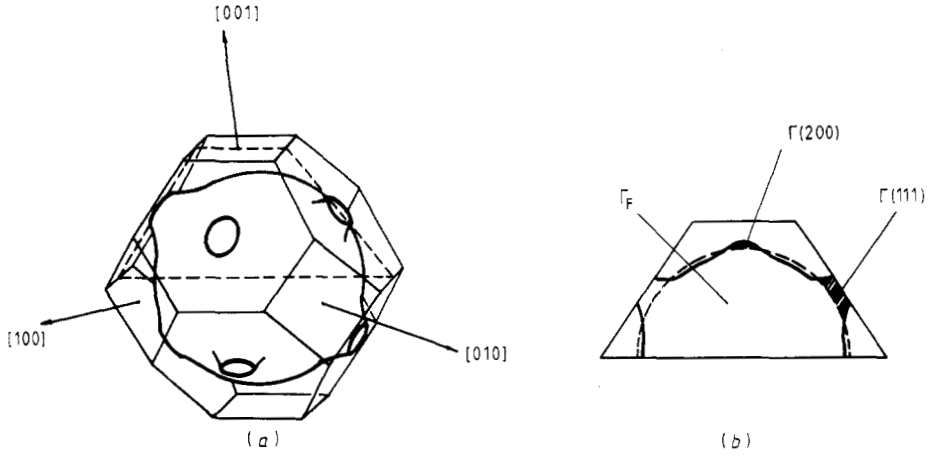

Figure 4. (*a*) The Fermi surface of a noble metal, (*b*) together with a section of it in the (110) plane. Distortions of sphericity are seen in the [111] and [200] directions.

contribution to the CF splitting as well as to the OL interaction. To obtain the conventional forms (1) and (2) for $\mathcal{H}_{\rm cov}$, we use the relation

$$\sum_{\sigma} f^{+}_{m\sigma} f_{m'\sigma} = \sum_{\kappa q} (2\kappa+1)(-1)^{m} \begin{pmatrix} 3 & \kappa & 3 \\ -m & q & m' \end{pmatrix} \sum_{i} C_{\kappa q}(\boldsymbol{r}_i) \Big/ 7 \begin{pmatrix} 3 & \kappa & 3 \\ 0 & 0 & 0 \end{pmatrix} \tag{10}$$

where the sum of one-electron spherical harmonics $C_{\kappa q}$ should be expressed in terms of Stevens operators.

For simplicity, the s and d conduction bands are considered to be independent and are described in the nearly-free-electrons and tight-binding approximations, respectively. The s-band isotropy affected by the lattice potential is damaged. Then, the contribution to (9) caused by the perturbation of free-electron wavefunctions is

$$\mathcal{H}^{(1)}_{\rm cov} = \sum_{\kappa q g m} \tfrac{2}{7} v(g) F_m(g) (-1)^{m} \begin{pmatrix} 3 & \kappa & 3 \\ -m & 0 & m \end{pmatrix} \begin{pmatrix} 3 & \kappa & 3 \\ 0 & 0 & 0 \end{pmatrix}^{-1} (2\kappa+1) C^{*}_{\kappa q}(\boldsymbol{g}) \sum_{i} C_{\kappa q}(\boldsymbol{r}_i) \tag{11}$$

$$F_m(g) = \sum_{k} \frac{V_{mk} V_{k+g,m}}{(\varepsilon_k - \varepsilon_{k+g})(\varepsilon_{+} - \varepsilon_k)} n_k .$$

$F_m(g)$ are calculated in the coordinate frame with $z \| \boldsymbol{g}$ using unperturbed energies and wavefunctions. Taking the non-sphericity of the Fermi surface into account in (9), we obtain

$$\mathcal{H}^{(2)}_{\rm cov} = -J_{\rm cov} \sum_{\kappa q g} \frac{\Gamma(g)}{\Gamma_{\rm F}} \frac{2\kappa+1}{4} C^{*}_{\kappa q}(\boldsymbol{g}) \sum_{i} C_{\kappa q}(\boldsymbol{r}_i)$$

$$J_{\rm cov} = \langle J_{\rm cov}(\boldsymbol{k}_{\rm F}, \boldsymbol{k}_{\rm F}) \rangle_{\Omega} \qquad J_{\rm cov}(\boldsymbol{k}, \boldsymbol{k}) = -\tfrac{2}{7} \sum_{m} \frac{V^2_{mk}}{\varepsilon_{+} - \varepsilon_k} \tag{12}$$

where $\Gamma_{\rm F}$ is the phase volume bounded by the Fermi surface, $\Gamma(g)$ is the phase volume occupied by the protuberance on the Fermi sphere in the $\boldsymbol{g}$ direction (figure 4). 'Necks'

in the [111] directions play the leading role here. The covalent contribution to the exchange constant J_{cov} is connected to the corresponding EPR g shift by the relation

$$\Delta g_{cov} = [(g_J - 1)g/g_J] J_{cov}\rho_s \tag{13}$$

where ρ_s is the one-spin density of s states at the Fermi level. Taking the energy perturbation in (9) into account, we obtain

$$\mathcal{H}^{(3)}_{cov} = J_{cov} \sum_{\kappa q g} \frac{v^2(g)}{\varepsilon_F x^2} \frac{2\kappa + 1}{8} C^*_{\kappa q}(g) \sum_i C_{\kappa q}(r_i) \sum_k c_{\kappa 0}(k) \frac{x_k}{x_k + \alpha_k} \frac{1}{\varepsilon_+ - \varepsilon_k} \tag{14}$$

$$x_k = g/2k \qquad x = g/2k_F \qquad \alpha_k = \cos\theta_k.$$

The effect of operator (14) proved to be insignificant, while the contribution to the CF parameters caused by (11) and (12) is

$$\begin{aligned} C_4^{f-s} &= -J_{cov}\{-\tfrac{7}{8}[\Gamma(111)/\Gamma_F] + 0.15\,\tfrac{3}{64}[v(111)/\varepsilon_F](\varepsilon_+/\varepsilon_F)\ln(1 + \varepsilon_F/\varepsilon_+)\} \\ C_6^{f-s} &= -J_{cov}\{\tfrac{13}{36}[\Gamma(111)/\Gamma_F] + \tfrac{3}{64}[v(111)/\varepsilon_F](\varepsilon_+/\varepsilon_F)\ln(1 + \varepsilon_F/\varepsilon_+)\}. \end{aligned} \tag{15}$$

Here ε_+ is taken relative to the Fermi energy ε_F. We have found the contribution of the 4f–s covalency to the OL coupling coefficients to be negligible.

The operator governing by the covalent coupling with the d band can be derived from (9) in the form

$$\begin{aligned} \mathcal{H}^{f-d}_{cov} = &\sum_{mm'\sigma} \sum_{jp} (\varepsilon_+ - \varepsilon^0_d)^{-1} V_{m,jp} V_{jp,m'} f^+_{m\sigma} f_{m'\sigma} \\ &+ \sum_{mm'\sigma} \sum_{jj'pp'} (\varepsilon_+ - \varepsilon^0_d)^{-2} V_{m,jp} V_{jp,j'p'} V_{j'p',m'} f^+_{m\sigma} f_{m'\sigma} + \ldots \end{aligned} \tag{16}$$

where ε^0_d is the d-band 'centre of gravity', the V-values are the inter-atomic hopping integrals, $|jp\rangle$ is the d orbital with angular momentum projection p at site j. In this mechanism, the impurity–ligand–impurity electron transfers produce the most important contribution. The processes described by (16) which are accompanied by the ligand–ligand transfers are not significant owing to strong angular dependence of the hopping integrals. Finally, we have

$$\begin{aligned} C_4^{f-d} &= -\tfrac{3}{32}(3V^2_{fd\sigma} + V^2_{fd\pi} - 7V^2_{fd\delta})/(\varepsilon_+ - \varepsilon^0_d) \qquad V^{(2)}_{5g} = (3 - q_{fd})X \\ C_6^{f-d} &= -\tfrac{2}{7}(V^2_{fd\sigma} - \tfrac{3}{2}V^2_{fd\pi} + \tfrac{3}{5}V^2_{fd\delta})/(\varepsilon_+ - \varepsilon^0_d) \qquad V^{(2)}_{5g} = 3(1 - q_{fd})X \\ q_{fd} &= -(R/V_{fd})(dV_{fd}(R)/dR)|_{R=d} \qquad X = \tfrac{10}{7}\alpha_J(V^2_{fd\sigma} + \tfrac{3}{2}V^2_{fd\pi})/(\varepsilon_+ - \varepsilon^0_d). \end{aligned} \tag{17}$$

For analysis of the hopping integrals in (17), it is convenient to use the relation [21]

$$V_{l_1 l_2 m}(R) \propto [(l_1 + m)!(l_1 - m)!(l_2 + m)!(l_2 - m)!]^{-1/2}(\Delta_1\Delta_2)^{1/2} R^{-(l_1 + l_2 + 1)}. \tag{18}$$

This is the case for strongly localised functions; Δ is the energy width of the corresponding state. From (18) it follows that the 4f–d covalency contribution is proportional to the d-band width Δ_d.

2.4. Effects of the impurity 5d states

The Hamiltonian needed for calculation of the 5d-states contribution may be written

$$\mathcal{H} = \mathcal{H}_{5d} + \mathcal{H}_s + \mathcal{H}_d + \mathcal{H}_{5d,s} + \mathcal{H}_{5d,d}$$

$$\mathcal{H}_{5d} = \sum_{\Gamma\alpha} \varepsilon^0_\Gamma a^+_{\Gamma\alpha} a_{\Gamma\alpha} + \mathcal{H}'_{OL} \qquad \mathcal{H}_s = \sum_k \varepsilon_k \hat{n}_k$$

$$\mathcal{H}_d = \sum_{jp} \varepsilon_d^0 d_{jp}^+ d_{jp} + \sum_{jj'pp'} V_{jp,j'p'} d_{jp}^+ d_{j'p'}$$

$$\mathcal{H}_{5d,s} = \sum_{\Gamma\alpha k} (V_{\Gamma\alpha,k} a_{\Gamma\alpha}^+ c_k + \text{HC}) \qquad \mathcal{H}_{5d,d} = \sum_{\Gamma\alpha jp} (V_{\Gamma\alpha,jp} a_{\Gamma\alpha}^+ d_{jp} + \text{HC}) \tag{19}$$

where ε_Γ^0 is the 5d–$\Gamma\alpha$-state energy in a cubic host ions' potential, $\Gamma = t_{2g}$ or e_g, and the $\mathcal{H}'_{OL}$ term has a form similar to (2) and describes the change in the lattice potential under distortion. The presence of the 5d-electron density in the impurity vicinity leads to the extra operator affecting the 4f electrons:

$$\mathcal{H}_{5d\text{–}4f} = \sum_{\kappa q \Gamma\Gamma' \alpha\alpha'} A_\kappa \langle \Gamma\alpha | C_{\kappa q}^* | \Gamma'\alpha' \rangle \langle a_{\Gamma\alpha}^+ a_{\Gamma'\alpha'} \rangle \sum_i C_{\kappa q}(\boldsymbol{r}_i)$$

$$A_\kappa = 2F^\kappa + (2\kappa+1) \begin{pmatrix} 2 & \kappa & 2 \\ 0 & 0 & 0 \end{pmatrix}^{-1} \begin{pmatrix} 3 & \kappa & 3 \\ 0 & 0 & 0 \end{pmatrix}^{-1} \sum_l \begin{pmatrix} 3 & 2 & l \\ 0 & 0 & 0 \end{pmatrix}^2 \begin{Bmatrix} 3 & 3 & \kappa \\ 2 & 2 & l \end{Bmatrix} G^l \tag{20}$$

where F^κ and G^κ are the Coulomb and exchange Slater integrals, respectively, and $\langle \ldots \rangle$ denotes the thermodynamic average with the Hamiltonian (19).

The contribution of operator (20) to the CF splitting can easily be found. For the regular lattice, $\langle a_{\Gamma\alpha}^+ a_{\Gamma'\alpha'} \rangle = \delta_{\Gamma\alpha,\Gamma'\alpha'} \tilde{n}_\Gamma$, then

$$C_4 = -\tfrac{1}{12}(\tilde{n}_t - \tilde{n}_e)[F^4 - \tfrac{11}{140}(9G^1 + 4G^3 + \tfrac{25}{121} G^5)]. \tag{21}$$

There is no 5d contribution to the C_6 parameter owing to the symmetry restrictions. The quantity $\tilde{n}_\Gamma$ may be treated as the 5d–$\Gamma\alpha$-state occupation number which arises because of the covalency effects. Provided that there is covalent coupling with the s band only, one can obtain

$$n_\Gamma = \tfrac{1}{2} - (1/\pi) \tan^{-1}(\varepsilon_\Gamma^0 / \Delta_{5d}) \tag{22}$$

where the 5d-level broadening $\Delta_{5d} = \pi \rho_s V_{\Gamma,k}^2$. Calculation of the covalency with ligands within the second order of the perturbation theory yields

$$n_\Gamma = \beta_\Gamma^0 = \frac{T_\Gamma}{(\varepsilon_\Gamma^0 - \varepsilon_d^0)^2} \qquad T_\Gamma = \sum_{jp} V_{\Gamma\alpha,jp}^2. \tag{23}$$

This is not correct in the case of strong covalent coupling. Therefore, we use the Green function method, allowing us to carry out partial summation of the perturbation theory series, to calculate the thermodynamic averages. The 5d–$\Gamma\alpha$-state Green function can be written as

$$G_\Gamma(\omega) = [\omega - \varepsilon_\Gamma^0 - \Sigma_\Gamma(\omega) + \text{i}0 \operatorname{sgn} \varepsilon_\Gamma^0)^{-1}$$

$$\Sigma_\Gamma(\omega) = \sum_{jp} V_{\Gamma\alpha,jp}^2 G_d(\omega) + \sum_k V_{\Gamma\alpha,k}^2 G_k(\omega) \tag{24}$$

$$= T_\Gamma(\omega - \varepsilon_d^0 + \text{i}0 \operatorname{sgn} \varepsilon_d^0)^{-1} - \text{i}\Delta_{5d} \operatorname{sgn} \omega.$$

In (24) the dispersion in the d band is neglected because the energy distance $\varepsilon_\Gamma^0 - \varepsilon_d^0 \simeq 5$ eV exceeds the d-band half-width $\Delta_d/2 \simeq 2$ eV. We obtain as the result

$$\tilde{n}_\Gamma = \text{Im}\left(\int_{-\infty}^{+\infty} \frac{\text{d}\omega}{2\pi} \exp(\text{i}0\,\omega)\, G_\Gamma(\omega) \right) = n_\Gamma + \tfrac{1}{2}[1 - (1 - 4\beta_\Gamma)^{1/2}](n_d - n_\Gamma)$$

$$n_\Gamma = \tfrac{1}{2} - (1/\pi) \tan^{-1}(\varepsilon_\Gamma / \Delta_{5d}) \qquad \beta_\Gamma = T_\Gamma / [(\varepsilon_\Gamma - \varepsilon_d)^2 + \Delta_{5d}^2] \tag{25}$$

$$T_t = 3V_{dd\sigma}^2 + 4V_{dd\pi}^2 + 5V_{dd\delta}^2 \qquad T_e = \tfrac{3}{2}V_{dd\sigma}^2 + 6V_{dd\pi}^2 + \tfrac{9}{2}V_{dd\delta}^2$$

where ε_Γ and ε_d are ε_Γ^0 and ε_d^0 energy levels changed because of the covalent repulsion; the renormalised covalent parameter is connected with the initial covalent parameter (23) by the relation $\beta = \beta^0/(1 + 4\beta^0)$; the V_{dd} are the impurity–ligand hopping integrals; the ligand state occupation number n_d equals unity.

This mechanism produces the OL interaction in two different ways: via the change in the lattice potential and via the modulation of the covalent coupling with ligands. When cubic symmetry is distorted, the averages $\langle a_\Gamma^+ a_\Gamma \rangle$ in (20) give increments proportional to the deformation, and off-diagonal averages arise. The lattice contribution to these variations, caused by the $\mathcal{H}'_{OL}$ term in the Hamiltonian (19), can be expressed as

$$\delta\langle a_{\Gamma\alpha}^+ a_{\Gamma'\alpha'}\rangle = \langle\Gamma'\alpha'|\mathcal{H}'_{OL}|\Gamma\alpha\rangle[(n_\Gamma - n_{\Gamma'})/(\varepsilon_\Gamma - \varepsilon_{\Gamma'}) - \beta_\Gamma/(\varepsilon_{\Gamma'} - \varepsilon_d) - \beta_{\Gamma'}/(\varepsilon_\Gamma - \varepsilon_d)]. \tag{26}$$

Using the explicit form of $\mathcal{H}'_{OL}$, i.e.

$$\mathcal{H}'_{OL} = \sum_{n\Gamma\alpha} v_\Gamma^{(n)} e_{\Gamma\alpha} C_{\Gamma\alpha}^{(n)}(r)$$

$$C_{3g\theta}^{(2)} = \tfrac{1}{2}(3z^2 - r^2)/r^2 \qquad C_{5g\zeta}^{(2)} = xy/r^2 \tag{27}$$

$$C_{3g\theta}^{(4)} = \tfrac{1}{2}(7z^4 - 4z^2r^2 - r^4 + 14x^2y^2)/r^4 \qquad C_{5g\zeta}^{(4)} = (7z^2 - r^2)xy/r^4$$

we find the 4f-electron OL parameters

$$\begin{aligned} V_{3g}^{(2)} = &-\tfrac{8}{49}A_2\alpha_J\{[\rho_e + 2\beta_e/(\varepsilon_e - \varepsilon_d)](v_{3g}^{(2)} + v_{3g}^{(4)}) \\ &+ [\rho_t + 2\beta_t/(\varepsilon_t - \varepsilon_d)](\tfrac{3}{4}v_{3g}^{(2)} - v_{3g}^{(4)})\} \\ V_{5g}^{(2)} = &-\tfrac{8}{49}A_2\alpha_J\{[\rho_t + 2\beta_t/(\varepsilon_t - \varepsilon_d)](\tfrac{3}{4}v_{5g}^{(2)} + v_{5g}^{(4)}) \\ &+ [(n_t - n_e)/(\varepsilon_e - \varepsilon_t) + \beta_e/(\varepsilon_t - \varepsilon_d) + \beta_t/(\varepsilon_e - \varepsilon_d)](v_{5g}^{(2)} - v_{5g}^{(4)})\} \end{aligned} \tag{28}$$

$$A_2 = 2F^2 - \tfrac{9}{7}(G^1 - \tfrac{11}{54}G^3 + \tfrac{125}{594}G^5) \qquad \rho_\Gamma = [\pi\Delta_{5d}((\varepsilon_\Gamma/\Delta_{5d})^2 + 1)]^{-1}.$$

Calculations similar to those in § 2.2 yield for the 5d-electron–lattice coupling coefficients

$$\begin{aligned} v_{3g}^{(2)} &= -(3Z\langle r^2\rangle/d^3)(1 + \sigma^{(2)} + \lambda_{3g}^{(2)}) \\ v_{5g}^{(2)} &= (3Z\langle r^2\rangle/d^3)(1 + \sigma^{(2)} + \lambda_{5g}^{(2)}) \\ v_{3g}^{(4)} &= -(185Z\langle r^4\rangle/24d^5)(1 + \sigma_{3g}^{(4)} + \lambda_{3g}^{(4)}) \\ v_{5g}^{(4)} &= -(25Z\langle r^4\rangle/2d^5)(1 + \sigma_{5g}^{(4)} + \lambda_{5g}^{(4)}). \end{aligned} \tag{29}$$

Here a part of the next-nearest surrounding spheres in $v_\Gamma^{(4)}$ is small: $\sigma_{3g}^{(4)} = -9.5 \times 10^{-2}$; $\sigma_{5g}^{(4)} = -6.2 \times 10^{-2}$. The screening factors were calculated above (see table 1).

Covalent coupling modulation provides

$$\delta\langle a^+_{\Gamma\alpha}a_{\Gamma'\alpha'}\rangle = [(n_\Gamma - n_d)/(\varepsilon_\Gamma - \varepsilon_d) - (n_{\Gamma'} - n_d)/(\varepsilon_{\Gamma'} - \varepsilon_d)][A_{\Gamma\Gamma'}/(\varepsilon_\Gamma - \varepsilon_{\Gamma'})]\delta T_{\Gamma'\alpha',\Gamma\alpha}$$

$$A_{\Gamma\Gamma'} = \tfrac{1}{2}[(1-4\beta_\Gamma)^{1/2} + (1-4\beta_{\Gamma'})^{1/2}]. \tag{30}$$

Then, the covalent contribution to the OL parameters is

$$\begin{aligned}
V^{(2)}_{3g} &= -\tfrac{8}{49}A_2\alpha_J\{[\rho_e - (n_d - n_e)/(\varepsilon_e - \varepsilon_d)][(Q^{(2)}_{3g} + Q^{(4)}_{3g})/(\varepsilon_e - \varepsilon_d)]A_{ee} \\
&\quad + [\rho_t - (n_d - n_t)/(\varepsilon_t - \varepsilon_d)][(\tfrac{3}{4}Q^{(2)}_{3g} - Q^{(4)}_{3g})/(\varepsilon_t - \varepsilon_d)]A_{tt}\} \\
V^{(2)}_{5g} &= -\tfrac{8}{49}A_2\alpha_J\{[\rho_t - (n_d - n_t)/(\varepsilon_t - \varepsilon_d)][(\tfrac{3}{4}Q^{(2)}_{5g} + Q^{(4)}_{5g})/(\varepsilon_t - \varepsilon_d)]A_{tt} \\
&\quad + [(n_d - n_e)/(\varepsilon_e - \varepsilon_d) - (n_d - n_t)/(\varepsilon_t - \varepsilon_d)] \\
&\quad \times [(Q^{(2)}_{5g} - Q^{(4)}_{5g})/(\varepsilon_e - \varepsilon_t)]A_{et}\}
\end{aligned} \tag{31}$$

$$Q^{(2)}_{3g} = 2(3 - q_{dd})Q^{(2)} \qquad Q^{(2)}_{5g} = 6(1 - q_{dd})Q^{(2)}$$

$$Q^{(4)}_{3g} = \tfrac{3}{4}(6 + 5q_{dd})Q^{(4)} \qquad Q^{(4)}_{5g} = \tfrac{9}{4}(5 + 2q_{dd})Q^{(4)}$$

$$Q^{(2)} = V^2_{dd\sigma} + V^2_{dd\pi} - 2V^2_{dd\delta} \qquad Q^{(4)} = V^2_{dd\sigma} - \tfrac{4}{3}V^2_{dd\pi} + \tfrac{1}{3}V^2_{dd\delta}$$

$$q_{dd} = -(R/V_{dd})(\mathrm{d}V_{dd}(R)/\mathrm{d}R)|_{R=d}.$$

We treat the splitting $\Delta_{et} = \varepsilon_e - \varepsilon_t$ between the t_{2g} and e_g states as caused by two effects. The initial splitting determined by the lattice potential was included in ε^0_Γ. It equals

$$\Delta^0_{et} = (5Z\langle r^4\rangle_{5d}/6d^5)(1 + \sigma_4 + \lambda_4). \tag{32}$$

Using the ion values for $\langle r^4\rangle_{5d}$ [20], we find that $\Delta^0_{et} = 0.42$ eV (Cu), 0.25 eV (Ag) and 0.28 eV (Au). However, the covalent repulsion of the levels reduces Δ^0_{et} because $T_t > T_e$ and leads to the disappearance of the final splitting. We believe that in fact there is no compensation, and this indicates that the use of the ion $\langle r^n\rangle_{5d}$-values is not correct. The more these states are extended, the greater the initial splitting is. Therefore, we treat Δ_{et} as a fitting parameter.

As mentioned above, when the impurity–ligand electron transfer is considered, the cross terms of $\langle a^+_{\Gamma\alpha}d_{jp}\rangle$-type arise in the charge density. It can easily be obtained that

$$\langle a^+_{\Gamma\alpha}d_{jp}\rangle = V_{jp,\Gamma\alpha}(n_d - n_\Gamma)/(\varepsilon_d - \varepsilon_\Gamma). \tag{33}$$

Then the electrostatic potential of the covalent charge on the 4f electrons is governed by the operator

$$\mathcal{H}_{5d\,cov} = 4\frac{n_d - n_\Gamma}{\varepsilon_d - \varepsilon_\Gamma}\sum_{\kappa q \boldsymbol{R} m}\langle r^\kappa\rangle_{4f}\langle 5dm|\frac{C_{\kappa 0}}{r^{\kappa+1}}|dm(R)\rangle V_{ddm}(R)C^*_{\kappa q}(\boldsymbol{R})\sum_i C_{\kappa q}(\boldsymbol{r}_i). \tag{34}$$

The relation

$$\langle 5dm|\,C_{\kappa 0}/r^{\kappa+1}\,|dm(R)\rangle = S_{ddm}(R)/(R/p)^{\kappa+1} \tag{35}$$

is valid when $m = 0$; here S_{dd} is the overlapping integral and p is parameter. Inserting (35) into (34), one can find that the covalent charges $Z'(R) = 4[(n_d - n_\Gamma)/(\varepsilon_\Gamma - \varepsilon_d)]S_{dd\sigma}(R)V_{dd\sigma}(R)$ are located on the impurity–ligand ties at a distance

Table 2. Crystal-field parameters for an Er impurity

Host	CF parameter (units)	Screened host ion field	Covalency effects 4f–d	Covalency effects 4f–s	Occupancy 5d	Covalency effects, 5d–d	Theory	Experiment
Cu	C_4 (K)	23	−15	−4	−52	14	−34	−36 [9], this work
Cu	C_6 (K)	3.4	−3.2	5.0	0	4.0	9.2	9.1 [9], this work
Ag	C_4 (K)	15	−11	−3	−58	5	−52	−52 [5]
Ag	C_6 (K)	1.7	−2.4	7.2	0	1.2	7.7	10.3 [5]
Au	C_4 (K)	18	−24	−6	−32	10	−34	−39 [4]
Au	C_6 (K)	1.8	−5.1	8.7	0	2.2	7.6	6.4 [4]

R/p from the RE ion. Their contribution to the 4f-electron–lattice interaction parameters is

$$C_4 = \tfrac{7}{32}Z'(d)\langle r^4\rangle/(d/p)^5 \qquad C_6 = \tfrac{39}{256}Z'(d)\langle r^6\rangle/(d/p)^7$$
$$V_{3g}^{(2)} = (2q_{dd}-3)B \qquad V_{5g}^{(2)} = 3(2q_{dd}+1)B \qquad B = Z'(d)\langle r^2\rangle\alpha_J/(d/p)^3. \tag{36}$$

3. Comparison with experiment

In this section we are mainly interested in the Er and Dy impurities. For the first time, the CF parameters for noble metals have been obtained from the magnetic susceptibility measurements in [2]. However, from these experiments, only the energy separation of the first excited level from the ground state have in fact been derived with satisfactory accuracy; these are $\Delta_{\Gamma_8-\Gamma_7} = 34$ K for **Ag**–Er, $\Delta_{\Gamma_8-\Gamma_7} = 1$ K for **Ag**–Dy and $\Delta_{\Gamma_8-\Gamma_7} = 19$ K for **Au**–Er. The Mössbauer spectrum analysis also is very arbitrary in the determination of the CF parameters. For example for **Cu**–Dy alloy it was found that $C_4 = -28 \pm 58$ K and $C_6 \simeq 20$ K [6]. In [4] it was shown that some information on the CF splitting can be obtained from the departure of the EPR linewidth thermal broadening from a linear $\Delta H = a + bT$ law and from g-value anisotropy at high magnetic field. Hence, only an analysis of various experimental data enables reliable determination of the CF parameters to be made. The EPR, magnetisation $M(H)$ and susceptibility $\chi(T)$ measurements in [5] for the **Ag**–Er and **Ag**–Dy systems have given $\Delta = 30 \pm 5$ K, $x = -0.33 \pm 0.02$ and $\Delta = 11.5 \pm 1$ K, $x = 0.53 \pm 0.01$, respectively (where x has the same meaning as in [12]). The corresponding values of C_4 and C_6 for an Er^{3+} ion in an Ag host are given in table 2.

Analysis of the experimental data available for Au and Cu can be greatly simplified assuming that Er^{3+} and Dy^{3+} ($J = \frac{15}{2}$) ions have similar values of C_4 and C_6 in the same hosts. Of course, the parameters change from one ion to another, in particular on the edges of the RE series (Ce and Yb), but our assumption seems to be reasonable for neighbouring ions (Er and Dy). This is substantiated by the data in [5]. Then the CF parameters can be determined when the Δ-values for both ions only are known. From the EPR measurements for the **Au**–Er system [4], Δ has been found to be 16 ± 6 K for $-0.4 \leqslant x \leqslant -0.2$. The ground state of the Dy^{3+} ion in an Au host is known to be the Γ_8 quartet [3]. This signifies that $x_{Er} \leqslant -0.34$. Thus, among the sets of parameters given in

[4], we can choose $\Delta = 16$ K and $x \simeq -0.36$. The corresponding values of C_4 and C_6 are presented in table 2.

In our previous work [9] the CF parameters for **Cu**–Er system have been derived from high-field magnetisation measurements. However, the obtained constants $W = 0.58$ K, $x = -0.4$, are doubtful because, as they are transferred on the Dy^{3+} ion, they produce $x_{Dy} = 0.64$ with the Γ_8 quartet in the ground state. At the same time, it is known [22] that the Dy^{3+} ground state in Cu is the Γ_7 doublet. We have carried out a detailed analysis and found that only the OL coupling parameters and the Δ-value can be obtained from high-field magnetisation measurements with good accuracy. Satisfactory adjustment to the experimental curves plotted in [9] (see figure 4 therein) is possible for $-0.4 \leqslant x \leqslant -0.2$. As a result, the new set of the CF parameters for the **Cu**–Er system (see table 2) is obtained.

When interpreting various experimental data in order to determine the OL parameters, one can be restricted by the second-order terms in the Hamiltonian (2). $V_\Gamma^{(2)}$ obtained from the EPR measurements on film samples [8] are given in table 3. We assume that they are greatly reduced in magnitude. The possible reasons for such a reduction have been discussed previously [9]. The values of the parameters derived from the magnetostriction [7] and EPR [9] measurements on bulk samples are also given in table 3. We think that the difference between them is connected with the change in elastic properties in the impurity vicinity. If the local deformation is related to the average deformation over a crystal as $e_{loc} = se_{av}$, then $V_\Gamma(\text{magn}) = V_\Gamma/s$ in the first case and $V_\Gamma(\text{EPR}) = V_\Gamma s$ in the second case. Hence $V_\Gamma = [V_\Gamma(\text{magn})V_\Gamma(\text{EPR})]^{1/2}$ is likely to be a more reasonable value.

As seen from table 2, the CF parameters do not change significantly through the noble-metal series. The point-charge model predicts greatly reduced magnitudes of the parameters ($C_4 \simeq 20$ K; $C_6 \simeq 3$ K) and an incorrect sign of C_4. On the contrary, the OL coefficients vary more considerably from host to host up to a sign change (see table 3). The interaction between the 4f electrons and trigonal deformations proved to be predominant while, within the point-charge model, $V_{5g}^{(2)} = -V_{3g}^{(2)} \simeq 10$ K. An account of screening in the form described in § 2.2 leads to the values of the constants listed in the third columns in tables 2 and 3.

Useful information needed to estimate the contributions from other mechanisms can be obtained from the EPR data. The total g shift in the metal is

$$\Delta g = \Delta g_{at} + \Delta g_{cov} + \Delta g_{5d}. \tag{37}$$

It is the sum of contributions from direct Coulomb interaction between the 4f and conduction electrons, from 4f–s covalent mixing and from 5d-state occupancy, respectively. Relaxation takes place through the three channels independently and the thermal broadening $b = \mathrm{d}(\Delta H)/\mathrm{d}T$ is

$$b = (\pi k/g\mu_B)(\Delta g_{at}^2 + \tfrac{1}{7}\Delta g_{cov}^2 + \alpha\,\Delta g_{5d}^2) \tag{38}$$

where k is the Boltzmann constant, μ_B is the Bohr magneton and α depends on the 5d-state energy structure. Using the equations obtained in [24] we find that within the t_{2g} model (the density of 5d-electron states at the Fermi level has mainly t_{2g} character)

$$\Delta g_{5d} = 3[g(g_J - 1)/g_J]A_0\rho_t + 4[g(2 - g_J)/g_J]A_1\rho_t = \Delta g_1 + \Delta g_2$$

$$b_{5d} = (\pi k/g\mu_B)(\tfrac{1}{3}\Delta g_1^2 + \tfrac{1}{2}\Delta g_2^2) \tag{39}$$

Table 3. Orbit–lattice coupling parameters for an Er impurity.

Host	OL coupling parameter (units)	Screened host ions field	Covalency effects		Occupancy		Covalency effects, 5d–d	Theory	Experiment		
			4f–d	4f–s	5dI	5dII			[9]	[8]	[23]
Cu	$V_{3g}^{(2)}$ (K)	−8.2	−0.9	0	0.6	−0.8	5.4	−3.9	−7.1	—	—
Cu	$V_{5g}^{(2)}$	6.8	−4.3	0	−4.4	−13.8	25.8	10.1	46	—	—
Ag	$V_{3g}^{(2)}$	−5.3	−0.6	0	3.8	1.3	2.5	1.7	6.3	0.5	2.0
Ag	$V_{5g}^{(2)}$	9.5	−3.1	0	−9.7	−1.2	11.8	7.3	52	2.4	5.2
Au	$V_{3g}^{(2)}$	−5.1	−1.4	0	7.2	−4.2	4.4	0.9	—	1.3	0.7 (Tb), 1.1 (Yb)[a]
Au	$V_{5g}^{(2)}$	14.4	−6.8	0	−15.8	−26.2	21.0	−13.4	—	−3.4	−3.8 (Tb), −5.3 (Yb)

[a] Here data for **Au**–Tb and **Au**–Yb systems are quoted because there is a lack of data for **Au**–Er.

Table 4. Experimental values of the EPR line g-shift and thermal broadening coefficient $b = d(\Delta H)/dT$ for an Er impurity, together with the results of theoretical treatment of these data according to equations (37)–(40).

	Theory						Experiment	
Host	Δg_{at} (10^{-2})	Δg_{cov} (10^{-2})	Δg_{5d} (10^{-2})	Δg (10^{-2})	b $(G\,K^{-1})$	$J_{5d}\rho_{5d}$ (10^{-2})	Δg (10^{-2})	b $(G\,K^{-1})$
Cu	1.3	−2.1	5.2	4.4	6.0	1.4	4 ± 1	6 [9]
Ag	1.3	−2.7	6.6	5.2	9.0	1.8	6.5 ± 1	
							8 ± 5	10.5 ± 1.5 [25]
								7 ± 1 [4]
Au	1.3	−3.2	3.0	1.1	2.7	0.35	3 ± 4	2.7 ± 0.5 [26, 27]

$$A_0 = \tfrac{2}{35}(3G^1 + \tfrac{4}{3}G^3 + \tfrac{50}{33}G^5) \qquad A_1 = \tfrac{1}{280}(4G^1 + \tfrac{2}{3}G^3 - \tfrac{50}{33}G^5).$$

If the 5d level is unsplit, then

$$\Delta g_{5d} = 5[g(g_J - 1)/g_J]A_0\rho_{5d} + 20[g(2 - g_J)/g_J]A_1\rho_{5d} = \Delta g_1 + \Delta g_2$$
$$b_{5d} = (\pi k/g\mu_B)(\tfrac{1}{5}\Delta g_1^2 + \tfrac{1}{10}\Delta g_2^2). \tag{40}$$

It should be noted that gold has a number of features in physical properties different from those of copper and silver. Au is characterised by a larger elastic modulus; the impurity Yb ion in Au has a magnetic moment; the Au d band is twice those of Cu and Ag. These peculiarities indicate an enhancement of d-orbital covalency effects in gold. Therefore, we believe that the 5d level of Er^{3+} in Au is greatly increased in energy and remains almost unsplit. Hence the 5d model (equation (40)) appears to be suitable for Au. On the contrary, splitting in Cu and Ag hosts probably occurs (let us assume these values to be 1 eV and 0.5 eV, respectively) and we treat the EPR data within the framework of the t_{2g} model (equation (39)). Assuming that $\Delta g_{at} = 0.013$ (as was done in [24]), we obtain Δg_{cov} and Δg_{5d} from equations (37)–(40). These values and experimental data used are listed in table 4. Now the covalent contribution (15) and (17) to the CF and OL parameters can be estimated. Knowing Δg_{cov} and using $\rho_s = 0.15\ eV^{-1}$/atom, one can obtain the exchange integral J_{cov}. We take the ε_F- and ε_d^0-values from the noble-metal band-structure calculations in [28] and the parameters for the Fermi surface from [29]. Other parameters employed are $v(111) = 1$ eV (it corresponds to the r_c-values chosen above), $\varepsilon_+ = 2$ eV and $q_{fd} = 6$; $V_{fd\sigma} = 0.14$ eV for copper. The results of the calculations are given in the fourth and fifth columns of tables 2 and 3. It turned out that, although the covalent contribution is remarkable, it is not as large as was assumed in [10]. It is interesting that 4f–d covalency is important only for C_4, while C_6 is mainly determined by the mixing of the 4f states with the s band. The large magnitude of C_6 for noble metals proved to be connected with anisotropy of the Fermi surface.

In table 4 the values of $J_{5d}\rho_{5d} = (g/g_J)(g_J - 1)(A_0\rho_{5d})$ are also given. For Au this quantity is much less than that for Cu and Ag. This supports the above assumption on the upward shift of the 5d level. Assuming that $\varepsilon_t = 1$ eV for the Ag host and $\Delta_{5d} = 0.5$ eV in all cases, we obtain the 5d-state structure of the Er^{3+} ion in the three metals (figure 5). The positions of the ε_d levels are also shown in figure 5. They are lower than the d-band 'centre of gravity' ε_d^0. The J_{5d}-value of 0.14 eV obtained is less than the J_{5d}-value of 0.4 eV calculated using atomic Slater integrals [20]. There are many reasons for

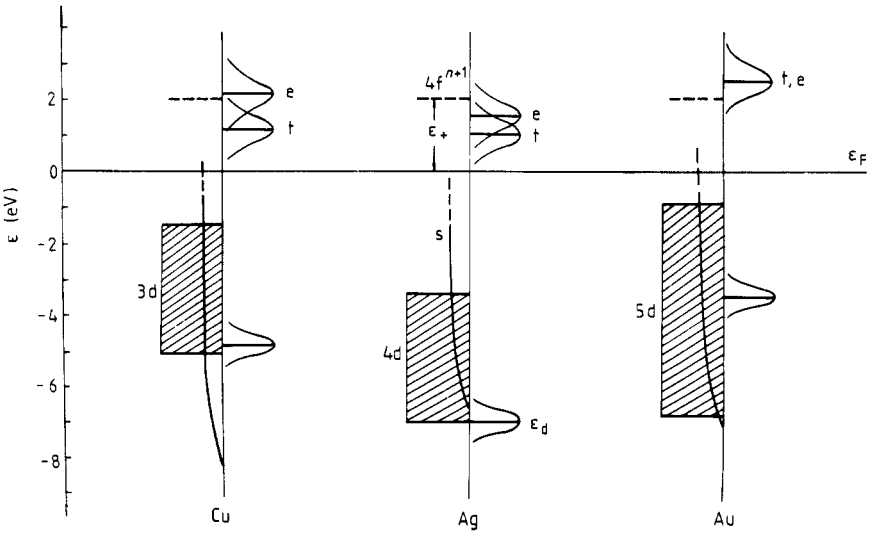

Figure 5. Electron state energy diagram of RE ion–noble metal system. The positions of the s and d bands, impurity 5d states with t_{2g} and e_g symmetries and ligand d levels ε_d, are shown. The energy of $4f^n s \rightarrow 4f^{n+1}$ excitation is also represented.

the exchange integral decrease in metal. In [30] the screening of the Coulomb 4f–5d interaction has been considered. At the same time, the reduction in the J_{5d} integral may be caused by the wider spatial extent of the 5d orbital. Using the atomic Slater integrals one can calculate the 5d contribution (21) to be $C_4 \simeq -20$ K. The smallness of the value obtained is due to strong compensation between direct and exchange contributions. The use in (21) of the values of G^k decreased by a factor J_{5d}^{at}/J_{5d}^{met} leads to $C_4 \simeq -100$ K. The integrals F^k in metals are likely to decrease too, but there is no experimental information on such estimations. We take $F^4 = 0.65F_{at}^4$ and $G^k = 0.35G_{at}^k$. The values of C_4 calculated with these magnitudes of the Slater integrals are presented in the sixth column of table 2. It is probable that the G^k (with different k-indexes) change differently upon a transition from an atom to metal. From [30], G^1 seems to be the most sensitive quantity to various approximations.

For the hopping integrals in (31), we use again the relation (18) and take $V_{dd\sigma} = 1$ eV for copper. The ion values for $\langle r^n \rangle_{5d}$ are employed in (29). The OL parameters calculated from equations (28) and (31) are listed in the sixth and seventh columns, respectively, of table 3. It should be noted that the fourth harmonics in the 5d-electron OL Hamiltonian play a remarkable role here.

To estimate the covalent-charge contribution (36), let us suppose that $V_{dd}S_{dd} \propto \Delta_d$. For copper, using the radial function $R_{3d}(r)$ [31], we obtain the values $S_{dd\sigma} = 4.75 \times 10^{-2}$, $p = 1.65$ and $Z' = 0.04$. In spite of the small covalent charge, its contribution is large enough (see the seventh column of table 2 and the eighth column of table 3).

Thus, using EPR data and some resonable physical arguments to estimate the contributions, we have succeeded in obtaining satisfactory description of the experimental constants of the RE ion–lattice interaction for all the hosts discussed. The sign change of $V_{5g}^{(2)}$ when one goes from silver to gold, which seemed to be surprising earlier [8, 23], proved to be mainly determined by the enhancement of covalency effects and the upward shift of the 5d level of the RE ion.

4. Conclusions

The analysis carried out in this paper shows that in metals the magnitude of the 4f-electron–lattice coupling is a result of the combined action of several equivalent mechanisms. One could not obtain a fair description of all interaction parameters by assuming that any one separate mechanism is predominant. The interaction has mainly a local character, covalency effects between the 4f and 5d states of the RE ion and d functions of the ligands being of great importance.

In spite of the fact that the theory is developed for noble metals, we believe that after a corresponding modification it can be applied to simple and transition metals.

References

[1] Turberfield K C, Passell L, Birgeneau R J and Bucher E 1970 *Phys. Rev. Lett.* **25** 752
[2] Williams G and Hirst L L 1969 *Phys. Rev.* **185** 407
[3] Davidov D, Orbach R, Rettori C, Tao L J and Chock E P 1972 *Phys. Rev. Lett.* **28** 490
[4] Davidov D, Rettori C, Dixon A, Baberschke K, Chock E P and Orbach R 1973 *Phys. Rev.* B **8** 3563
[5] Oseroff S, Passeggi M, Wohlleben D and Schultz S 1977 *Phys. Rev.* B **15** 1283
[6] Kikkert P J and Niesen L 1980 *Hyperfine Interact.* **8** 135
[7] Creuzet G and Campbell I A 1981 *Phys. Rev.* B **23** 3375
[8] Pela C A, Suassuna J F, Barberis G E and Rettori C 1981 *Phys. Rev.* B **23** 3149
[9] Garifullin I A, Farzan T O, Khaliullin G G and Kukovitsky E F 1985 *J. Phys. F: Met. Phys.* **15** 979
[10] Barnes S E, Baberschke K and Hardiman M 1978 *Phys. Rev.* B **18** 2409
[11] Duthie J C and Heine V 1979 *J. Phys. F: Met. Phys.* **9** 1349
[12] Lea K R, Leask M J M and Wolf W P 1962 *J. Phys. Chem. Solids* **23** 1381
[13] Borg M, Buisson R and Jacolin C 1970 *Phys. Rev.* B **1** 1917
[14] del Moral A, Echenique P M and Corrales J A 1983 *J. Phys. C: Solid State Phys.* **16** 4637
[15] Christodoulos F and Dixon J M 1987 *J. Phys. C: Solid State Phys.* **20** 5537
[16] Anderson P W 1961 *Phys. Rev.* **124** 41
[17] Deniszczyk J 1988 *J. Phys. F: Met. Phys.* **18** 797
[18] Harrison W A 1980 *Electronic Structure and the Properties of Solids* (San Francisco: Freeman)
[19] Freeman A J and Watson R E 1962 *Phys. Rev.* **127** 2058
[20] Starostin N V, Gruzdev P P, Pashnina E P and Ganin V A 1975 *Crystal Spectroscopy* (Moscow: Nauka) p 216
[21] Andersen O K, Klose W and Nohl H 1978 *Phys. Rev.* B **17** 1209
[22] Altshuler T S, Kharakhashyan E G, Kukovitskii E F and Zaripov M M 1977 *Phys. Status Solidi* b **80** K109
[23] Campbell I A and Creuzet G 1985 *J. Phys. F: Met. Phys.* **15** 2559
[24] Lacueva G, Levy P M and Fert A 1982 *Phys. Rev.* B **26** 1099
[25] Chui R, Orbach R and Gehmann B L 1970 *Phys. Rev.* B **2** 2298
[26] Tao L J, Davidov D, Orbach R and Chock E P 1971 *Phys. Rev.* B **4** 5
[27] Chock E P, Davidov D, Orbach R, Rettori C and Tao L J 1972 *Phys. Rev.* B **5** 2735
[28] Fleck U, Wonn H and Ziesche P 1980 *Phys. Status Solidi* a **61** 447
[29] Ashcroft N W and Mermin N D 1976 *Solid State Physics* (New York: Holt-Sanders)
[30] Christodoulos F and Dixon J M 1987 *Phys. Lett.* **124A** 437
[31] Watson R E 1960 *Phys. Rev.* **119** 1934